

## Experiment Report Form

**The double page inside this form is to be filled in by all users or groups of users who have had access to beam time for measurements at the ESRF.**

Once completed, the report should be submitted electronically to the User Office using the **Electronic Report Submission Application:**

<http://193.49.43.2:8080/smis/servlet/UserUtils?start>

### ***Reports supporting requests for additional beam time***

Reports can now be submitted independently of new proposals – it is necessary simply to indicate the number of the report(s) supporting a new proposal on the proposal form.

The Review Committees reserve the right to reject new proposals from groups who have not reported on the use of beam time allocated previously.

### ***Reports on experiments relating to long term projects***

Proposers awarded beam time for a long term project are required to submit an interim report at the end of each year, irrespective of the number of shifts of beam time they have used.

### ***Published papers***

All users must give proper credit to ESRF staff members and proper mention to ESRF facilities which were essential for the results described in any ensuing publication. Further, they are obliged to send to the Joint ESRF/ ILL library the complete reference and the abstract of all papers appearing in print, and resulting from the use of the ESRF.

Should you wish to make more general comments on the experiment, please note them on the User Evaluation Form, and send both the Report and the Evaluation Form to the User Office.

### **Deadlines for submission of Experimental Reports**

- 1st March for experiments carried out up until June of the previous year;
- 1st September for experiments carried out up until January of the same year.

### **Instructions for preparing your Report**

- fill in a separate form for each project or series of measurements.
- type your report, in English.
- include the reference number of the proposal to which the report refers.
- make sure that the text, tables and figures fit into the space available.
- if your work is published or is in press, you may prefer to paste in the abstract, and add full reference details. If the abstract is in a language other than English, please include an English translation.

Fig.2 GI-SAXS pattern for the **AuL4C12** film, compared with the bulk small-angle powder diffraction pattern

A previously-measured powder SAXS pattern of **AuL4C12** is shown in Fig 2, displaying six diffraction peaks. The GI-SAXS measurement show far more structural information. As shown in Figure 2(b), the GISAXS pattern can be indexed well on a rhombohedral lattice with space group  $R\bar{3}m$ . The orientation is of the fibre type, i.e. with the domains cylindrically averaged around the  $[1\bar{1}1]$  axis which is perpendicular to the substrate surface – see also Figure 2c. The unit cell parameters are  $a = 80.0 \text{ \AA}$ ,  $c = 35.4 \text{ \AA}$ . With the diffraction peaks indexed and space group determined, we proceeded to reconstruct the electron density map using the measured diffraction intensities. Since the structure has an inversion centre, one can write

$$E(x, y, z) = \sum_{h,k,l} \sqrt{I(h,k,l)} \cos[2\mathbf{p}(hx + ky + lz) + \mathbf{f}_{h,k,l}] \text{ where the phase angle } \mathbf{f}_{h,k,l} \text{ for each diffraction order}$$

is either 0 or  $\pi$ . However, as the phase angle can not be directly determined from the X-ray data, the choice of phase combination was made on the basis of the physical merits of the electron density map, with the help of existing knowledge of the system. The right phase combination gives well defined low and high density regions, due to the high contrast in electron density between gold nanoparticles and their surroundings. As only a few peaks were observed for each mesophase all possible phase combinations were examined, and the best solution was decided on the basis of the electron density maps and histograms obtained.

The resulting 3-d map in Figure 3(a) shows that the gold nanoparticles arrange in columns along the  $[001]$

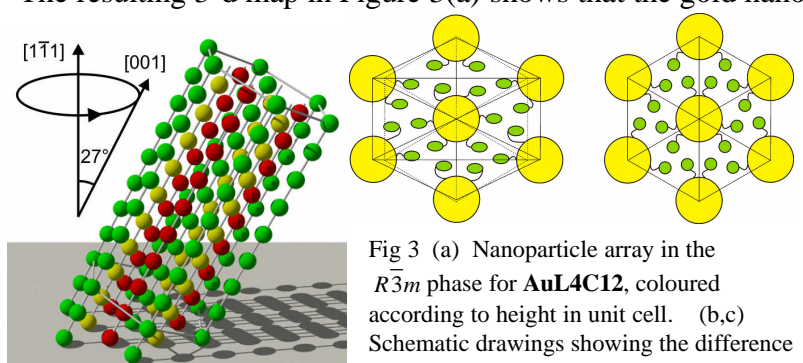


Fig 3 (a) Nanoparticle array in the  $R\bar{3}m$  phase for **AuL4C12**, coloured according to height in unit cell. (b,c) Schematic drawings showing the difference in the ordering of ligands for the rectangular (30°C) and hexagonal (90°C) phases.

direction. The columns pack on a simple triangular lattice, clear when viewed along the  $[001]$  direction.

For **AuL4C6**, the nanoparticles with the shorter hexylthiol co-ligand chains, a plane group  $c2mm$  with  $a = 74.4 \text{ \AA}$ ,  $b = 40.8 \text{ \AA}$  was obtained for 30-80°C. At 90 °C and 100 °C the lattice is 2D hexagonal,  $p6mm$ , with  $a = 41.0 \text{ \AA}$ . 2D electron density maps of both the rectangular and hexagonal phases were reconstructed. The resulting structures are

shown schematically in Figures 3(b,c). The large circles are the projections of the nanoparticle columns, surrounded by the nematogenic rod-like ligands viewed along their long axis (small circles or ellipses). The arrangements of the columns in the two phases are similar: the centred rectangular phase transforms to the hexagonal by shrinkage in the  $a$  direction until the  $a/b$  ratio drops to  $\sqrt{3}$ . The reconstructed maps indicate that the nanoparticles in **AuL4C6** also form columns as in **AuL4C12**. However, only two dimensional long range ordering of column axes exists in **AuL4C6**.

The mesophase structure of both **AuL4C12** and **AuL4C6** can be described as consisting of columns of nanoparticles surrounded by a sheath of axially aligned mesogens. While with dodecylthiol chains in **AuL4C12** the interparticle gap along the column is kept at  $16.5 \text{ \AA}$  (Figure 4a), by changing to hexylthiol in **AuL4C6** the gap is reduced to a mere  $4.8 \text{ \AA}$  in the  $p6mm$  phase (Figure 4b). This work demonstrates that highly ordered superlattices of metal nanoparticles other than those expected from mere packing of spheres can be created by coating the particles with a laterally attached nematogenic ligand. The results give the first rules on which to base future designs of more complex lattices with a view to build self-assembled metamaterials. Work on new gold nanoparticle superlattices is in progress. We have a paper in draft form to be submitted shortly.

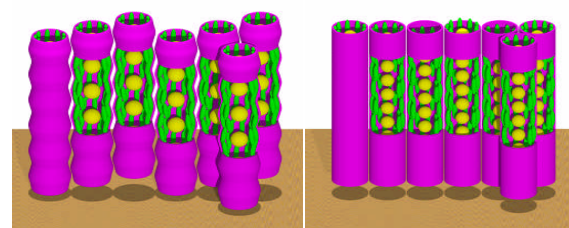


Figure 4 Schematic models of the (a) rhombohedral phase in **AuL4C12** and (b) the hexagonal columnar phase in **AuL4C6**; yellow: gold nanoparticles, green: mesogens.

## References

- [1] Rockstuhl, C. & Scharf, T. A metamaterial based on coupled metallic nanoparticles and its band-gap property. *J. Microscopy* **229**, 281-286 (2008).
- [2] Rockstuhl, C., Lederer, F., Etrich, C., Pertsch, T. & Scharf, T. Design of an Artificial Three-Dimensional Composite Metamaterial with Magnetic Resonances in the Visible Range of the Electromagnetic Spectrum. *Phys. Rev. Lett.* **99**, 017401 (2007).
- [3] Whetten, R.L. et al. Nanocrystal gold molecules. *Adv. Mater.* **8**, 428-433 (1996).
- [4] Cseh, L. & Mehl, G.H. Structure-property relationships in nematic gold nanoparticles. *J. Mater. Chem.* **17**, 311-315 (2007).